The Production and Electrospinning Application of Novel Collagen Materials

Kiran Mistry

Submitted to Swansea University in fulfilment of the requirements for the Degree of Master of Science by Research in Tissue Engineering & Regenerative Medicine

Swansea University

2023

Swansea University
Prifysgol Abertawe

Abstract

Arthritis affects millions of people worldwide. Deteriorating the smooth cartilage layer and causing repeat build of scar tissue and subsequent breakdown. Collagen is the main biological material that forms the extra cellular matrix of cartilage and provides its strength. Electrospinning is a versatile technique and highly adjustable which is why it has seen a rise in popularity. The use of collagen in tissue engineering in order to produce scaffolds has been widely explored with great strides in collagen blends and application. However, they all suffer from the use of harsh solvents such as 1,1,1,3,3,3-Hexafluoro-2-Propanol (HFP) or 2,2,2-trifluoroethanol (TFE), which denature collagen into gelatine, which has none of the favourable characteristics of collagen. In this study, it has been determined that a neutral solvent, PBS can be used and mixed with Single Alpha-Chain Jellyfish collagen to produce electrospun fibres with an average of 0.759µm in diameter using the electrospinning technique. With the process parameters of 20 kV, 0.05 ml/hr flow rate and a distance between collector and tip of 16 cm.

Declarations

This work has not previously been accepted in substance for any degree and is not being concurrently submitted in candidature for any degree.

Signed - K. Mistry

Date - 07/06/2023

This thesis is the result of my own investigations, except where otherwise stated. Other sources are acknowledged by footnotes giving explicit references. A bibliography is appended.

Signed - K. Mistry

Date - 07/06/2023

I hereby give consent for my thesis, if accepted, to be available for electronic sharing

Signed - K. Mistry

Date - 07/06/2023

The University's ethical procedures have been followed and, where appropriate, that ethical approval has been granted.

Signed - K. Mistry

Date - 07/06/2023

Table of Contents

Contents

Acknowledgements

I would like to thank Dr Chris Wright for his unwaivering patience and profound knowledge in the subject. You have helped when I hit sticking points in my research and helped me see it to the end.

I would also like to thank my family for believing in my and giving me emotional support when times got dark and immoveable. Your belief and constant encouragement helped me get to where I am today. To you I owe everything.

0.1 Table of Figures

0.2 Table of Tables

0.3 Abbreviations

- Extra Cellular Matrix – ECM
- 1,1,1,3,3,3-Hexafluoro-2-Propanol - HFP
- 2,2,2-trifluoroethanol – TFE
- Phosphate Buffer Saline – PBS
- Di - Deionised
- Scanning electron Microscopy - SEM
- High Depth of Field Microscopy - HDoF
- Fourier-Transform Infrared Spectroscopy - FTIR
- X-Ray Diffraction - XRD
- Ultimate Tensile Strength - UTS

1. Introduction

New medicines are being developed every day in order to improve quality of life. Recently exciting developments in the field of tissue engineering has been paving the way for harnessing the body's own repair mechanisms to improve healing . In normal wound healing the body follows its own healing process which in many cases results in scar tissue. However, with the use of tissue engineering techniques this can be optimised by growing that tissue and applying it where it needs to go. By using the patient's own stem cells there is also no risk of rejection because the cells used come from the patient's own body.

Past iterations of this type of procedure required artificial materials to be introduced into the implant site. Such as a coronary graft for a heart bypass (Aroesty, 2015). The largest issue plaguing artificial implants is immune rejection. This is due to the introduction of a foreign object into the body causing the body to fight and try and get rid of it. This in turn causes more distress and pain to the patient. Regarding the heart bypass vessel. The tubing can work well for several years but due to the artificial nature of the graft the seal may not be perfect. In regard to that, the body will continue to heal over that opened space and cause another atrial occlusion.

In the case of arthritis cartilage repair is compromised with the condition affecting millions of adults around the globe. Cartilage has been found to heal, however it scars over very easily. This can cause joint pain, which in turn makes arthritis worse. Collagen is a key component of cartilage and has been extensively investigated in tissue-engineering for scaffold fabrication and implantation. Collagen can be a great material to work with for cartilage repair and a scaffold may be used to return a cartilage surface back to its smooth hyaline characteristics (Yu et al., 2022).

Based on previous analysis of literature and the effects of harsh solvents on collagen denaturation (Zeugolis et al., 2008) this study will examine the use of a novel collagen material (single alpha chain) to improve the electrospinning of collagen materials for tissue engineering.

1.1 Aims & Objectives

1.1.1 Aims

The aim of this thesis is to optimise the application, characterisation and production of electrospun single alpha-chain collagen. To make sure the aim is met a number of objectives must be addressed on the way:

1. How collagen has been electrospun in the past, and how can this process be improved.
2. What precautions and procedural requirements must be taken in order to reduce or stop collagen denaturisation.
3. Construct a detailed procedure for the electrospinning of collagen.
4. Introduce hydroxyapatite into the electrospinning process to enhance the mechanical properties of the collagen scaffolds. The mechanical failure of collagen scaffolds is often a limitation of these procedures within tissue engineering.
5. The influence of the addition of hydroxyapatite into the scaffolds will be characterised using mechanical testing.

2. Background Information & Literature Review

2.1 Tissue Engineering & Regenerative Medicine

Tissue engineering is a subject that centres on the development of biomaterials. These biomaterials can be derived from a few fundamental elements: cells, scaffolds and biologically communicating factors. These fundamentals can be used in conjunction with each other to forward the advancements in medicine and produce native tissue *in vivo* for repair or replacement of damaged tissues or complete organs. S. Agarwal comprehensively states that 'Tissue engineering makes use of scaffolds to provide support for cells to regenerate new extra cellular matrix which has been destroyed… Without stimulating any immune response' (Agarwal et al., 2008) Therefore, the ideal tissue engineering scaffold would be the culmination of bioactive growth factors; the patients' own cells all on a biocompatible material.

Inside the body a natural extra cellular matrix (ECM) is secreted from a group of cells. This ECM provides a support structure for those cells and also helps actuate cell signalling. Therefore, an ECM can be considered the scaffold for cells in a tissue, providing additional structure and a template for cells to populate. Therefore, a tissue engineered scaffold should mimic the ECM of a tissue to support the development of new cells as they build back their own ECM. This process starts with the fabrication of the scaffold from an array of different techniques and possible materials. The next step is for cell seeding, this takes the final scaffold and floods it with a solution of new cells which can come accompanied with growth factors to aide in cell maturity and assemble into a native tissue.

Regenerative medicine includes the use of tissue engineering and researches the use of the body's own healing mechanism with help from foreign biological materials. This incorporation will encourage cell regrowth and rebuild tissues and organs back to health.

2.2 Scaffold Fabrication

To fabricate a scaffold for tissue engineering, the aim is to directly mimic native extra cellular matrix in order to support and promote new tissue formation. As previously mentioned in section 2.1 the scaffold must be biocompatible so as not to induce an immune response. The implanted scaffold is intended to be a temporary structure, maintaining some residual strength of the structure and allow space for new cells to penetrate and propagate

through the body's natural healing process. With certain mimicry the newly implanted ECM can become enveloped in the cells and become part of the newly formed tissue. Therefore, a structural scaffold should be close enough to allow full biocompatibility and absorption to the tissue without degrading into toxic by-products. Furthermore, the result should strike a balance between mechanical strength all while maintaining mimicked porosity. There are a few methods that can form such scaffolds and can be tested then implemented rapidly. Electrospinning is one of the many techniques for tissue engineering scaffold fabrication which also includes: porogen leaching, solvent casting, gas foaming, phase separation, drawing, self-assembly, template synthesis and rapid prototyping. These various techniques all have their uses; however, the versatility of electrospinning makes it a favourable choice for application in Tissue engineering and regenerative medicine. A comparison of a few of the above techniques table 2.1 compares some of the more popular methods namely:

Process	Advances	Scalability	Repeatability	Convenience	Process Control
Electrospinning	Laboratory & commercial	Yes	Yes	Yes	Yes
Template Synthesis	Laboratory	No	Yes	Yes	Yes
Phase Separation	Laboratory	No	Yes	Yes	No
Self-Assembly	Laboratory	No	Yes	No	No
Drawing	Laboratory	No	Yes	Yes	No

Table 2-1 – A comparison between common scaffold fabrication techniques. (Ramakrishna, S. et al., 2005)

Electrospinning, template synthesis, phase separation, self-assembly and drawing.
The table above highlights the limitations of other methods and brings forth the merits of electrospinning. With complete control of the process and scale, this technique is of great use for tissue engineering and regenerative medicine.

2.2.1 Template synthesis

Template synthesis is a method of fibre fabrication that can use a metal oxide membrane with nano-scale diameter pores throughout – this is similar to an extrusion die plate used to make electrical cables. The use of template implies that the fibres will be uniform in nature and follows a guide or mould in order to obtain the desired measurements and design, this template also gives an indication of the repeatability of the process. Where a pressure is applied to a liquid polymer that allows the medium to pass through to the membrane into a solidifying solution. Upon contact with the solution, the fibres become independent with diameters determined by the membrane pores. For example, a water buffer can be used against a hydrophobic polymer such as the technique used by Feng et al, to push the desired material through a template screen with nano-scale pores into a solidifying solution (Feng et al., 2002). This technique can be summarised by the diagrams in figure 2-1:

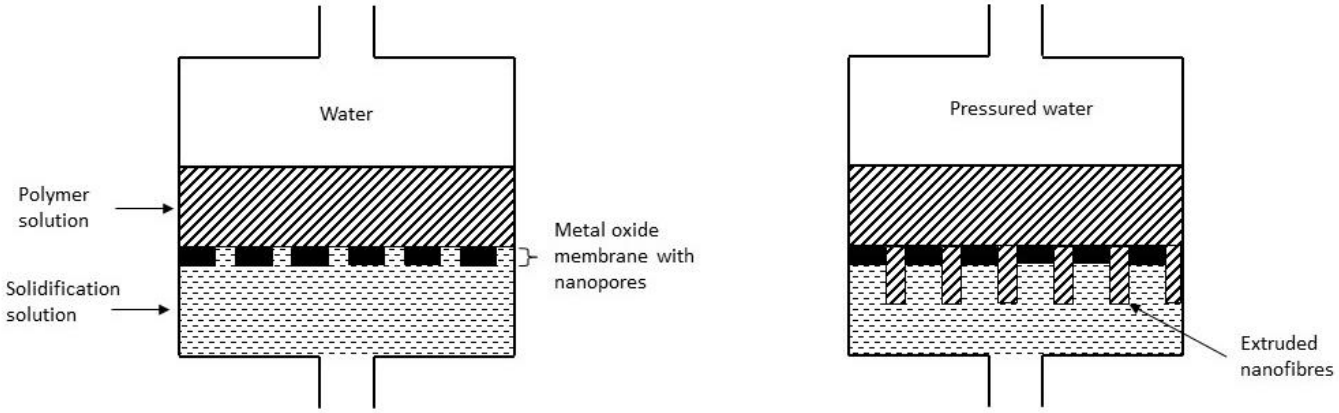

Figure 2.1 - Simple schematic of nanofibre extrusion via template synthesis

2.2.2 Phase separation

Regarding phase separation, it starts by mixing a solvent with a polymer before becoming a gel. As the name suggests, the process involves the separation of the gel and the solvent in the mixture due to physical incompatibility. The solvent is later extracted leaving the remaining gel phase behind. The process consists of 5 steps that take it from solution to porous polymer scaffold: polymer dissolution, gelation (cloud point), freezing, solvent extraction and freeze drying. This can be described as such below (Hua et al., 2002):

1. Weighted Poly(L-lactic acid) (PLLA) (3, 4.5, or 6 wt%) was put in a mixture of 1,4-dioxane and water as varying concentrations (84.5/15.5, 87/13 and 88.5/11.5, wt/wt). The solution was then heated to 63 °C until dissolved.
2. The solution was heated to 15 °C which is above the measured cloud-point temperature then dipped into a water bath that was preheated to the quenching temperatures (20, 25, 30, or 35 °C). The solution was then left on the bath for varying times (1, 2, 5, 10, 30, or 60 min) to observe the coarsening effect of the final material.
3. The sample was then immersed in liquid nitrogen to be frozen.
4. Using an electric knife, a small hole was cut to allow the remaining solvent to be drained out.
5. Finally, the frozen scaffold was freeze dried at −77 °C and 7 mm Torr for 3 days.

These steps yielded a highly porous scaffold of PLLA. A simplified version of this process is shown in figure 2-2:

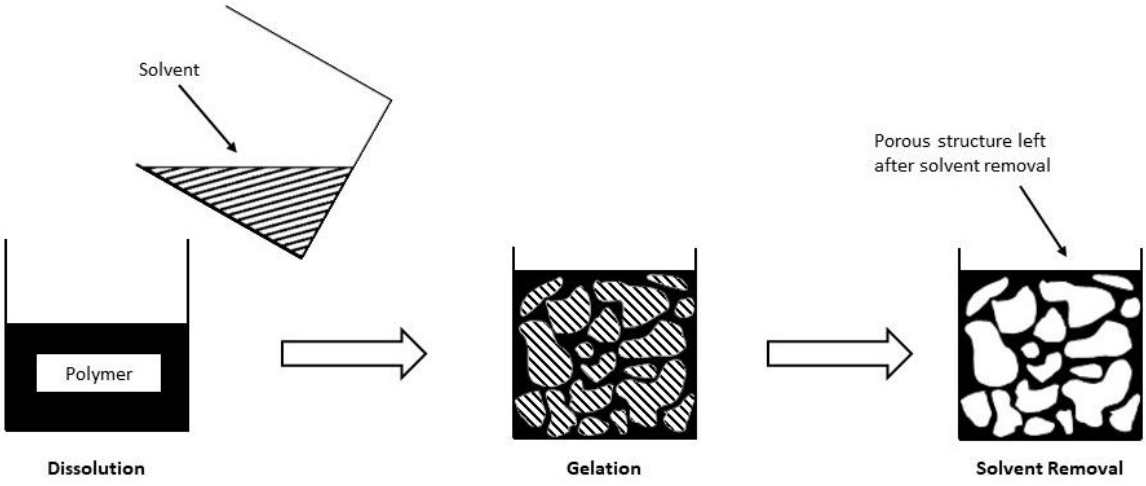

Figure 2.2 - Simplified diagram showing the workflow of phase separation.

2.2.3 Self assembly

The self-assembly process refers to the building of nanofibres from smaller molecules without the influence of external energy and interference. It has been noted that self-assembling processes show promise in forming cartilaginous tissue that is reminiscent of native tissue (Athanasiou et al., 2013). The mechanism for generic self-assemble used the intermolecular forces that pulled the smaller molecules together and shape themselves into

the more desirable macromolecular nanofibre. A method noted by (Lee et al., 2017) uses a substrate of nonadherent culture, agarose, which is used to support cellular seeding and prevent early cell attachment. This separation then encourages cell-cell interactions and facilitating in specific assembling. The spacing within the structure increases the free energy available and therefore encourages certain interactions from cell-cell. The free energy available on the surface of the cells is critical as no external stimuli is needed thus defining the self-assembly process.

2.2.4 Drawing

Drawing as a process can be compared to pulling fibres from a spool of thread. A simplified view of the process can be seen in figure 2-3.There are several ways but in general it can be broken down into three distinct steps (Ondarçuhu et al., 1998): (1) On an applicable substrate, a droplet of polymer solution is applied, (2) A micropipette is moved towards a droplet of polymer solution making contact with the edge of the droplet and (3) via backward motion of the micropipette the fibre is pulled from the droplet at a pre-determined rate. The final cross section of the fibre can be alters depending on the draw velocity, evaporation speed of the used solvent and exact material composition.

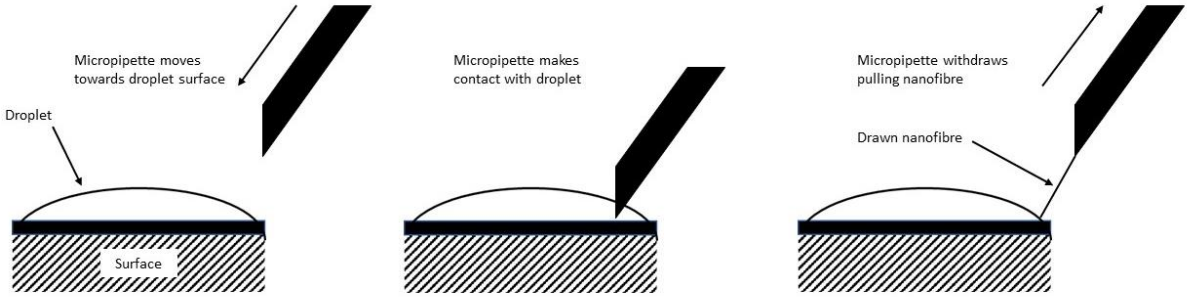

Figure 2.3 - Simplified look at drawing nanofibre from droplet of polymer solution.

The production of fibres through drawing is considered slow due to, in many cases, one micropipette being implemented at a time and a finite amount of polymer present. However, recent developments have included a micromanipulator (Bajáková et al., 2011). It has been designed solely for this fabrication method. In principle, the micromanipulator will provide a continuous supply of the polymer in exact quantities to the probe which is in

contact with the positioner. The probe is then lowered onto the substrate which initiates the drawing process from the probe – drawing the polymer fibre at a precise speed.

2.3 Electrospinning

2.3.1 Process & Variations

Electrospinning is a scaffold fabrication method which involves the extrusion of nanofibres from melts or a solution using high repulsion due to a high intensity electrical field. Those extruded fibres fly onto a grounded collection plate, hardening within the distance between the needle tip and the plate. A general electrospinning setup consists of syringe pump containing polymer solution or melt material, a high voltage power supply (typically 1-50kV) and a collection place in the range from 1-30 cm. These are the fundamental components of the spinner which are also shown below:

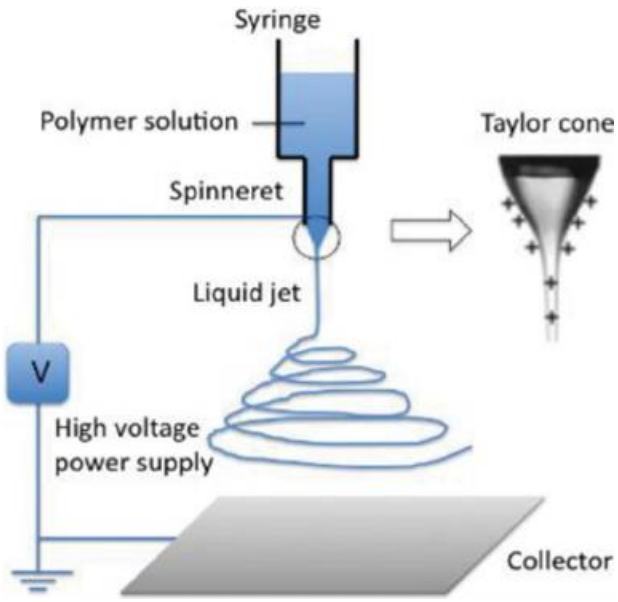

Figure 2.4 - Basic Electrospinning setup with single needle and stationary grounded plate. (Sapountzi et al., 2015)

The functioning of the electrospinner starts with a solution being fed through a conductive capillary, with a blunt end, in order to maintain a droplet at the end by its own surface tension. This capillary or needle is directed at the grounded collector plate. The needle is connected to the high voltage power supply in order to act as an electrode to charge the solution inside. The charge being applied to the capillary makes like charges repel each

other on the surface which directly opposes the solutions surface tension. This repulsion changes the shape of the pendant like droplet to a Taylor cone (Taylor et al., 1969).

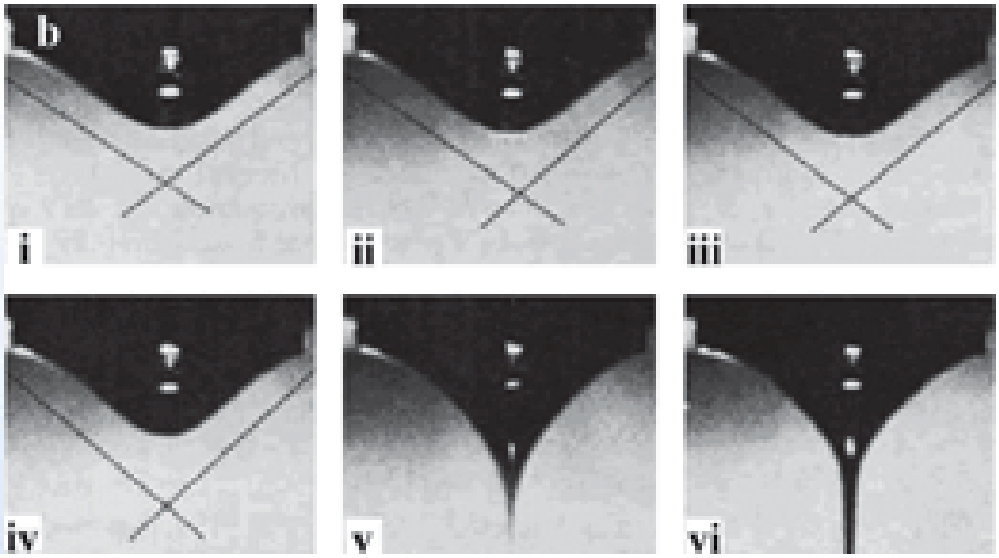

Figure 2.5 - Step by step formation of Taylor cone jet from liquid drop. (Di et al., 2011)

At a critical voltage, the electrostatic forces within the solution overcome its own surface tension initiating a single jet to extrude in the direction of the grounded collection plate. The solution must be viscous enough to remain as a single stream and not break up into droplets due to Rayleigh instabilities (Yarin et al., 2001). Rayleigh instabilities is a result of surface tension of the pulled solution which leans towards minimising the surface area of the solution by forming into individual droplets rather than staying together as a continuous cylinder of material. Once the jet is ejected, it undergoes a whipping motion which incidentally thins and dries the fibres as it travels towards the collector plate. Therefore, on the plate is a single mass of randomly oriented and dispersed fibres of the dried solution. This is a basic outlook on the electrospinning process; realistically there are many combinations of collectors, orientations and spinnerets, which can all be changed to produce different effects. This enables any user to tailor the equipment to their specific needs, in turn making the process desirable with its allowed versatility.

2.3.1.1 Core/Shell Production

The core/shell application involves the formation of fibres composed of different polymers as seen in Figure 2.6.

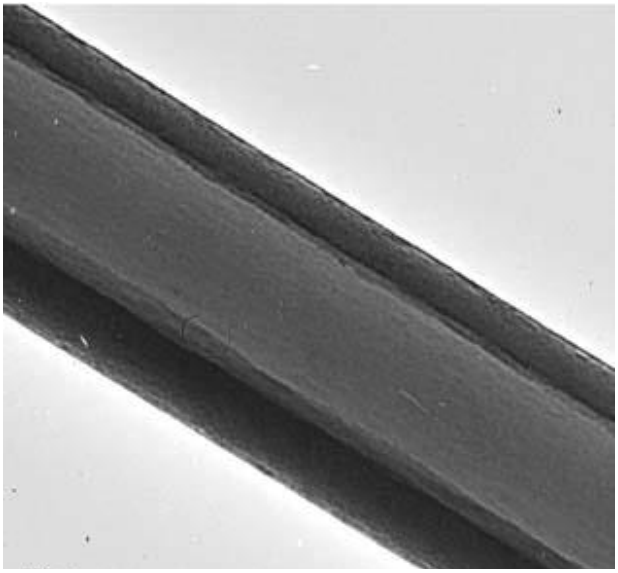

Figure 2.6 - TEM micrograph of electrospun PGS-PLLA/PLLA core/shell nanofibers. (Yi et al., 2008)

This creates a fibre composition with one polymer in the centre and another wrapped around that core which is comparable to an electrical wire. This composite nanofibre design enable the resulting scaffold to exploit the positive qualities of both polymers which gives more freedom in adapting the scaffold for a specific use. A summation can be made that this combination is applicable for tissue engineering scaffolds focussed around specific drug delivery (Huang et al., 2006).

Figure 2-6 shows an example of a core/shell electrospun fibre, with the lighter colour representing the core of the spun fibre and the darker section the sheathe. There are two main processes in which a core/shell design can be achieved: the use of immiscible material blends or use of a compound spinneret.

Compound electrospinning was first introduced by (Sun et al., 2003) With the design of a needle with two entry points and a single exit. This compound spinneret kept the source polymers separate from each other until the tip where the polymers join as they form the Taylor cone. From that point, onwards the process is largely similar to simple single needle electrospinning. As the electrostatic forces rice, formation of a composite Taylor cone

arises. With continued exposure, the cone is pulled into a continuous fibre of core/shell characteristics.

2.3.1.2 Needleless

As for most electrospinning processes, a needle is utilised to introduce the material solution into the system. The use of a needle allows for a single point of charge to be applied making it easier for jet initiation. However, in the case of needleless electrospinning, the applied voltage is set to a bath of the solution rather than a single point. The now charged bath of polymeric material can form multiple jet initiation sites from the free liquid surface in turn producing several fibre jets at once (Niu, Lin and Wang, 2011). The initiation of multiple jets makes for increased productivity whilst improving the cost effectiveness of the process; this is highly desirable for the commercial applications.

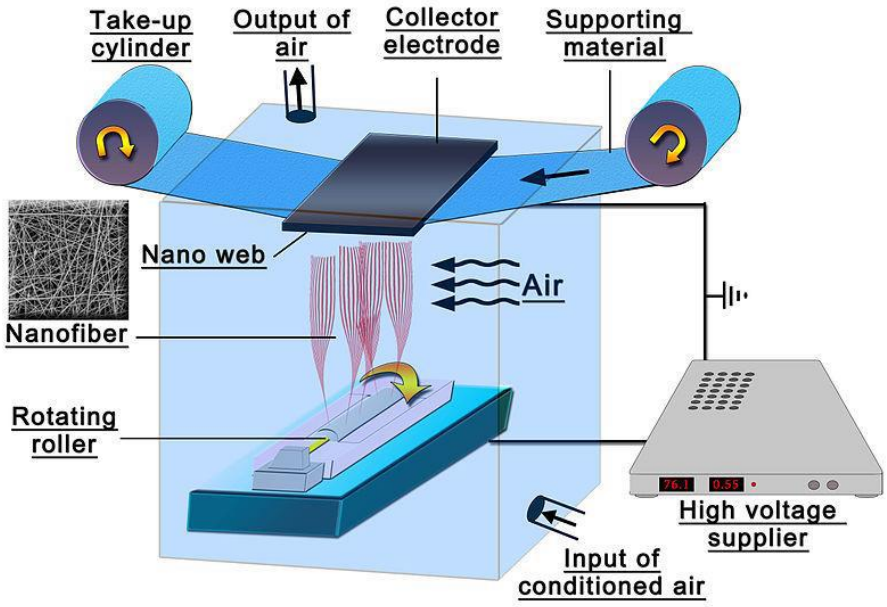

Figure 2.7 - Diagram of Elmarco Nanospider™ free liquid surface electrospinning setup (Yalcinkaya et al., 2015)

As shown in the above figure, a commercialised needleless electrospinner is manufactured by Elmarco namely the 'Nanospider™'. This system consists of a solid rotating drum bathed in the polymer solution which helps keep a fresh supply of polymer whilst maintaining multiple jet sites. This system can also be adjusted to use multiple wires in place of the rotating drum to induce more jets.

Needleless electrospinning shows great promise for the introduction into the industrial market. With the used of the electrospinning technique across a wire or multiple extraction

points on a bath. The scale up possibilities are there to be exploited. While the limitation of conventional electrospinning comes by way of material deliverance via needle ends. A needleless approach strips away that factor. Allowing the electrostatic force to run freely within the solution to be drawn. Natural Taylor cones would form along the surface allowing a near limitless amount of initiation sites. It also allows a continuous production approach by way of a feed roller providing a fresh substrate to deposit the spun fibres onto as well as an exponentially larger solution capacity allowing for greater spun durations.
Modern machines such as the Nanospider can also maintain a fixed atmosphere within the chamber which can influence how the non-woven mat reacted with the electrostatic force and can also affect drying times when in contact with the substrate.
The scope for this technology is broad with applications in many types of industry. With its emergence of continuous or batch production technologies, the future of non-woven fabricated scaffolds is here.

2.4 Effects of Electrospinning Process Parameters

As a technique for scaffold fabrication, electrospinning is extremely customisable. Allowing its user the freedom to adjust a variety of parameters to achieve fibres with specific features. These adjustable aspects of electrospinning are put into three categories: Process, Solution and Ambient. Process parameters includes adjusting the electrospinning system such as the amplitude of applied voltage and the distance between the spinneret tip and grounded collection plate. On the other hand, solution parameters centre on the characteristics of the solution used. This includes the concentration and molecular weight. Finally, ambient parameters cover the room temperature and atmospheric humidity. These can affect fibre morphology; however, these do not cause a profound change to the result. The balance of these parameters is imperative in order to achieve fibres with the correct characteristics and repeatable results.

2.4.1 Process Parameters

Process parameters encompasses the direct manipulation of the electrospinning system. These are the type of collector, distance from spinneret tip to collector, applied voltage and solution flow rate. These parameters can be changed during electrospinning runs to

improve fibre morphology and collection result. Applied voltage and collector distance provide the most distinguishable changes to the electrospinning result.

2.4.1.1 Applied Voltage

The electrospinning process relies on the electrostatic force between the spinneret and collector and can only start once that force crosses a threshold for the solution. The voltage applied must rise high enough to form a Taylor cone and initiate fibre formation however not high enough to cause electrospraying. The optimum voltage exists in a finite range; however, this is dependent on the viscosity and surface tension of the solution. It has been observed that an increased voltage outside of optimum ranges can initiate more beading of the final fibres (Deitzel et al., 2001) however; other effects have been observed that claim otherwise. A study by Yuan et al. concluded that an increased applied voltage produced fibres with reduced diameter and minimal beading due to higher electrostatic force on the solution. Another study found that the higher voltage draws more material from the spinneret tip with thicker fibres as a result (Zhang et al., 2005). With mixed conclusions on the effect of voltage on fibre diameter, it is hard to determine it as a major contributor for fibre diameter change.

2.4.1.2 Collector Distance

To achieve the desired fibre characteristics, it is necessary to find the optimum distance between the grounded collection plate and the spinneret tip. This optimum can be attained through trial and error although caution should be practiced and not create a distance too small. This could initiate an electrical arch and short out the system – requiring a system restart.

The distance creates a flight path for the extrusion to occur and in turn gives the solution time to dry. Altering this will create more time for the solvent to dry creating a dry extruded fibre however, too short of a distance will not give enough time for that to occur. Beading can also occur if the flight distance is too short (Li & Wang et al., 2013).

2.4.2 Solution Parameters

Solution parameters are to be considered when preparing the material for electrospinning.. This involves the primary solute (in case of this study, collagen), the solvent and any additives to alter the electrospun result. Some common parameters are the concentration of solute, volatility of solvent, viscosity, conductivity, surface tension and molecular weight. The effect of conductivity and concentration are explored, as the primary solute will remain constant for the purpose of this study.

2.4.2.1 Conductivity

The conductivity of the solution is determined by the solute and solvent used. With the addition of other compounds, like salt, which is an ionically bonded compound, those ions can become free ions with the addition of an electrical charge. This addition of free ions within the solution increases conductivity from solutions, which lack natural electrical conduction or have a high surface tension to overcome. This higher conductivity can have an effect on fibre diameter by increasing the bending instability due to the availability of competing electrostatic forces. This initiates an excess in jet whipping elongating the fibres at an unpredictable rate (Petrik & Maly et al., 2009). Zong et al (2002) observed that increased conductivity of a solution leads to the reduced formation of beading on the fibre deposition.

2.4.2.2 Concentration

The change in concentration of a solution can have profound effects on the process. A solution concentration too low can lead to poor fibre formation or the effect of electrospraying or a large amount of beading onto the collector plate (Deitzel et al., 2001). On the other hand, a high concentration solution can cause an issue with flow through the spinneret and increases the risk of in process coagulation. A solution concentration within a suitable range can provide suitable solution flow where a certain viscosity is reached and other variables are adjusted to account for given concentration. A high concentration solution forms a more viscous solution. This can be ideal when larger diameter fibres are desired; this result is cause by the increased weight of solution resisting the electrostatic force applied to the bulk solution.

2.4 Collagen

The integration of natural polymers in tissue engineering has allowed not only the mimicry of ECM structure but also the inherent nature of the polymer delivers a recognisable and physiologically relevant platform for cell proliferation and tissue growth. The use of naturally derived polymers is vastly encouraged. The current state of tissue engineering has explored the use of, collagen, fibrinogen, gelatine, elastin and other blends. Within the human body, the ECM of most tissues is comprised of collagen fibrils this includes skin, cartilage, bone, nerves and blood vessels. The abundance of collagen highlights its role in

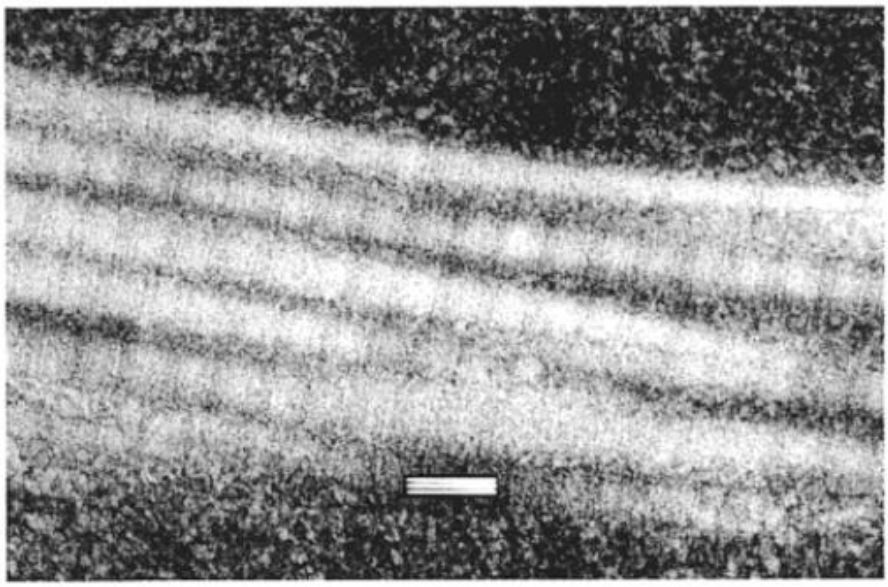

Figure 2.8 - TEM of the electrospun type I calfskin collagen. Electroprocessed fibers exhibit the 67 nm banding typical of native collagen (inserted scale bar 100 nm). (Matthews, 2001)

maintaining biological and structural integrity for native ECMs. It is also noted to undergo dynamic remodelling to maintain proper physiological function (Petreaca et al., 2014). Collagen as a biological material is unique with it present in the majority of tissues and by weight, composing 30% of the human body(Chaffey et al., 2003). With this wide-spread use of collagen, there are 16 different types however, there are some universal details which accompany all types: right-handed triple helix and 67 nm banding. The triple helical structure comes from polar interactions between segments of the protein forming its tertiary three-dimensional structure. The banding is derived from a repeating motif between α chains(Ramakrishna et al., 2005) in the coiled structure. This repeating motif creates the characteristic banding seen in figure 2-8:

This is exclusive to collagen. The variety of collagen types can complicate the view of which is the best for any intended biomaterial use, however, each has been largely characterised. Below is a table of the four most researched and useful types of collagen for tissue engineering; I, II, III and V.

Type	Chain Composition	Details	Localisation
I	$[\alpha1(I)]_2[\alpha2(I)]$	300 nm fibril length, uniform 50 nm diameter, 70-90% of all collagen in the body, precisely 1050 amino acids.	Bone, skin, tendon, blood vessels, fibrocartilage, cornea, etc.
II	$[\alpha1(II)]_3$	67 nm banding periodicity, less than 80 nm diameter, exclusively in cartilaginous tissues. Closely associated with water, proteoglycans, glycoproteins and non-collagenous proteins.	Articular cartilage, intervertebral disc, vitreous humor, etc.
III	$[\alpha1(III)]_3$	67 nm banding periodicity, 30-130 nm diameter, for granulation tissue, precursor for type I.	Skin, muscle and associated with type I.
V	$[\alpha1(V)]$ $[\alpha2(V)]$ $[\alpha3(V)]$	N-term globular domain consisting of small fibres.	Most interstitial tissue associated with type I.

Table 2-2 - List of fibrous Collagen types, chain composition, details and locality of each type.(Zhang et al., 2005)

Type I is most abundant in tendon rich environments such as rat tails, which were first isolated by (Chandrakasan et al, 1976) along with its characterisation. Its ultra-structure allows enormous tensile strength by bundling together aligned collagen fibrils into bigger fibres then combining those fibres into tendon tissue. This makes collagen type I, gram for gram, stronger than steel (4).

On the other hand, and the main focus of this study is type I single alpha chain collagen. As displayed in table 2.2, type I collagen is localised in tendons, bone, skin and blood vessels. The application for such a material is versatile. It is flexible and elastic in nature allowing for

a wide range of uses. . In comparison to type II, which by use, has a more rigid responsibility in the body enabling for major load bearing situations such as knees, elbows and the spine.

2.4.1 Electrospinning Collagen

The use of collagen as a tissue engineering scaffold material has been explored for a number of years. There are many techniques involving electrospinning where collagen was the main natural material in question. However, in many cases, the collagen was exposed to harsh solvents or processes which initiate denaturisation. The most common include: 1,1,1,3,3,3-Hexafluoro-2-Propanol (HFP) (Rho et al., 2006) or 2,2,2-trifluoroethanol (TFE) (Zhang et al., 2005). However, with prior information, it is known that the use of fluoroalcohols not only denature proteins but has an alternative effect of lowering the denaturation temperature of said proteins (Hong & Hoshino et al., 1999). Yang et al (2008) states that 45% of collagen was lost using volatile fluoroalcohols such as, HFP and TFE.

Reports in which collagen is dissolved in a solution of HFP or TFE state that the resulting collagenous structures are soluble in water, blood or other tissue fluids (Kidoaki et al.,2005). Since collagen is insoluble in water, these reports must be initiating a denaturing change to the morphology allowing them to dissolve in aqueous solution. Gelatine on the other hand is water-soluble and can be derived from the breakdown of original collagen fibrils (Veis et al., 1961) it is safe to assume that the original collagen has gone through the degradation process.

This information urges the use of a less volatile solvent to be used in the electrospinning process when dealing with collagen. In order to preserve the triple helical structure and characteristic D banding.

2.4.2 Collagen Blends

When it comes to the internal matrix of a collagen-based material, the components are rarely 100% collagen. In fact, collagen can interact and be combined with a multitude of organic and inorganic materials to add functionality and versatility. The use of additives to the process can also rise the success rate of cell seeding onto the material and create nucleation sites for cell adhesion.

There are various established collagen blends used for electrospinning. These can include collagen-elastin (Buttafoco et al., 2006), collagen-polycaprolactone which has been established for vascular tissue engineering (Buttafoco et al., 2006) and fibrinogen fibres allow native collagen deposits to grow through natural growth (McManus et al., 2006). These blends can also include additives such as hydroxyapatite which has been found to be a promising material for bone regeneration. The combination of collagen and hydroxyapatite is bioactive and can induce bone tissue formation. At nanoscale, bone can be summarised as collagen reinforced with hydroxyapatite (Fratzl et al., 2004). These blends can help mitigate some of the denaturing factors brought on from volatile solvents. Moreover, they can be used to provide promising properties for applications in drug delivery or scaffold applications.

3. Materials & Methods

3.1 Materials

The phosphate buffer saline (PBS) was obtained from ThermoFisher Scientific, phosphoric acid (for analysis 85% wt% solution in water) obtained from ACROS Organics, calcium nitrate tetrahydrate (97+%) from Alfa Aesar and ammonium hydroxide solution (ACS Reagent 28-30%) was obtained from Honeywell. All sampling solutions of Single Alpha-Chain Jellyfish collagen were dissolved in PBS. A 3ml syringe was used in conjunction with a 1.2 blunt end needle, which applies the start of the bridge for the electrospinning process. The needle was placed in a Cole Parmer step motor pump for 0.1 ml/hr flow rate adjustment. Finally, the power supply is a Brandenburg Regulated High Voltage Power Supply. This power supply was chosen because it has three equipped safety switches – all switches must be depressed in order for power to flow through the system.

Without the use of HFP or TFE a higher concentration is necessary to ensure the electrostatic forces can pull the solution from the spinneret tip to the collector plate. Initial protocols were based on the use of high viscosity to ensure large diameter and strong fibres for eventual mechanical testing. Following solutions were made with the inclusion of hydroxyapatite with varying %weight to explore the boundary of electrospun mats. Preparation of hydroxyapatite was explored using the method explored by Jing et al (2012). This was done with a stoichiometric ratio of [Ca]/[P]=1.67. This combined with the materials listed above provide an insoluble precipitate ready for drying and addition to collagen/PBS solutions. Solution variations come in two forms: first principal solution, which consists of only single alpha-chain collagen and PBS with the other being the same collagen/PBS solution with different concentrations of hydroxyapatite.

First principal solutions were made up from one part PBS with 25% by weight of collagen. 25% was chosen due to the balance it provided in solution stability when in storage and during the electrospinning process. At lower weight percentage of collagen, the solutions were too thin and could not be influenced by the electrostatic pull enacted but the electrospinning equipment. In actuality the solution would not react to the electrostatic force until a threshold was reached and the media would spray out to the collector plate. On the other-hand, above 25% by weight of collagen testing became a swift problem. The

concentration was high enough to cause coagulation issues in the needle which prevented further non-woven mat fabrication. At 25% under exposure to the elements during the electrospinning process, sufficient time could be spent adjusting flow parameters before further testing could be initiated. The concentration of hydroxyapatite was determined by the weight of collagen in the solution. In turn the range explored was between 10-20% by weight of collagen.

3.2 Electrospinning

The electrospinning was done using a traditional needle to collection plate method. Using a 3ml syringe equipped with 1.2 blunt end needle. Approximately 2 ml of solution was drawn into the syringe and pushed free of air. The full syringe placed on the Cole Parmer step motor pump. Clips were placed on the spinneret tip and collection plate in order to create the electrostatic force for electrospinning to occur. The Brandenburg power supply can apply a range of voltages from 0-30 kV. The surrounding material in the chamber was non-conductive in order to maintain direct flight between the Taylor cone formed at the spinneret tip to the collector plate.

For initial test purposes and calibration of test solution, the distance from spinneret tip to collection plate remained constant with applied voltage being altered. This was used to determine the effect of applied voltage on the solution and flow rate. The importance during this phase was to ensure that threshold voltage was exceeded in order for fibre deposition however not high enough for electrospraying. Aluminium foil was used as the collection material because of its availability and abundance.

Initial runs involved searching for Taylor cone expression at the end of the needle with first expression seen at 10 kV. Distance between the collector plate and spinneret tip remained constant for the tests to ensure consistent fibre morphology and even comparison. The range of voltages was between 10-22 kV. Anything below 10 kV resulted in little electrostatic pull on the solution with no pull towards the collector plate. With voltages exceeding 22 kV, the spraying effect increases over a wide area on the Aluminium collector plate. At some distances, a higher voltage can cause the system to short circuit due to the electricity jumping from spinneret tip to collector. The pump, syringe and collector plate

were all contained in a non-conductive covering in a temperature & humidity regulated laboratory.

3.3 Hydroxyapatite

Hydroxyapatite was explored in part due to its abundance in bone and zero need to bio activate. There are several different methods to form hydroxyapatite particles in the laboratory starting with a stoichiometric ratio between Calcium and Phosphorus of [Ca]/[P]=1.67. A technique explored by Teng et al (2008) and Zhang et al (1997) were used to synthesise Hydroxyapatite. Briefly the stoichiometric weight of both phosphoric acid and calcium nitrate tetrahydrate were dissolved in DI water separately. Slowly the Phosphoric acid solution was poured into the calcium nitrate tetrahydrate solution with stirring. After a minute, ammonium hydroxide was added to keep the pH level at 10. The end solution then is kept at 50°C under vigorous stirring for 5 hours then covered and aged for 24 hours at room temperature. Following, it is centrifuged at 2500 rpm and washed with DI water four times.

The final treatment of the hydroxyapatite was then adjusted. There are three methods explored including air-drying, freeze drying and sintering. Sintering involved placing dried precipitate into a furnace with a 30°C ramp up per minute to 1100°C and maintained for 5 hours. This process was involved as to induce rod like crystal formation in the final particles. Once a dry powder was obtained, the hydroxyapatite was crushed with a pestle and mortar in order to get uniform sizing throughout.

3.4 Fibre Characterisation

3.4.1 Scanning Electron Microscopy (SEM)

Fibre morphology was characterised using a Zeiss Evo Scanning Electron Microscope. Operating within a variable and high-pressure vacuum at 10-20 kV. The samples were mounted onto Aluminium stubs and observed at magnification of 150x to 3000x. Image magnification varies throughout however, where relevant it was the same in order to compare across platforms such as the use of SEM in tandem with High Depth of Field imaging. The results gained at lower magnifications proved beneficial to see fibre orientation. Allowing a macro view for sample analysis. Although, during the initial stages of

development, the magnifications used were very high. This was necessary to ensure that fibres were formed and not sprayed during electrospinning. Images captured were taken for further image analysis using ImageJ.

3.4.2 High Depth of Field Light Microscopy (HDoF)

The hydroxyapatite particles were assessed using a Keyence VHX1000 operating at either 200x magnification or 1000x magnification. The samples were pressed into carbon tape on aluminium stubs to gain a contrast between the background and particles. The images from this technique were assessed for particle size and consistency with ImageJ.

3.4.3 Image Analysis

The fibre diameters were assessed for each separate mat and average collated from each one. Using the ImageJ software and the included measuring tool, the diameter of 30 explicit fibres were taken. The scale bar in the corner was used to determine the units of measurement on each photo to ensure consistent measurements and reliable data.

3.4.4. Micro Tensile Testing

During sample generation, thick mats were obtained which could be tested on the Deben In-Situ Micro Tensile Tester. The load cells can range from 2-200N with progression steps down to 0.1 mm/minute. The samples were cut using a scalpel to a length of 30 mm and width of 15 mm to ensure consistent and comparable results.

4. Results & Discussion

4.1 Calibration

Initial electrospinning runs produced a number of effects ranging from dense electrospun deposition to light spraying with large droplets on the collector plate. The initial runs were as follows:

Material	Flow rate (ml/hr)	Voltage (kV)	Distance (cm)
25% Single Alpha-Chain Collagen/1x PBS	0.05	15	11
25% Single Alpha-Chain Collagen/1x PBS	0.05	16	11
25% Single Alpha-Chain Collagen/1x PBS	0.08	18	11
25% Single Alpha-Chain Collagen/1x PBS	0.08	20	11
25% Single Alpha-Chain Collagen/1x PBS	0.08	14	11
25% Single Alpha-Chain Collagen/1x PBS	0.06	12	11
25% Single Alpha-Chain Collagen/1x PBS	0.06	10	11

Table 4-1 - Principal Electrospinning runs with varying voltage to initialise spray versus fibre formation.

The distance of these initial runs remained constant with changes occurring to the applied voltage and flow rate. Some of these initial tests were plagued by beading with some fibre formation or just electrospraying. Calibration testing formed the base for understanding how collagen solutions react to the electrospinning process. In table 4.1, it has been noted that initial testing was maintained at 11cm from needle tip to collector plate. However, with an increased voltage the flow rate of the solution needed to be adjusted accordingly.

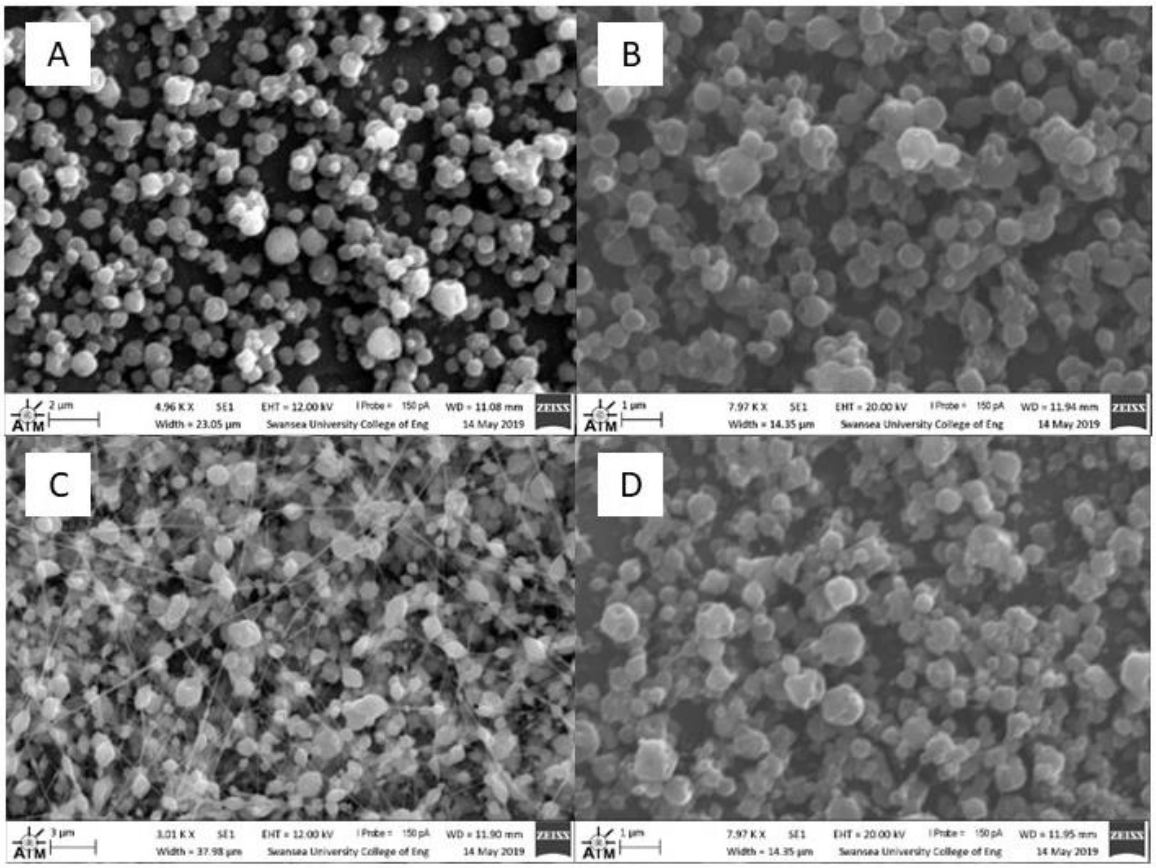

Figure 4.1 - SEM images of fibre and beading formation of electrospinning calibration using 25% Monomeric Collagen with 1x PBS at different applied voltages: A – 10 kV at 0.06 ml/hr. B – 12 kV at 0.05 ml/hr. C – 15 kV at 0.05 ml/hr. D – 16 kV at 0.05 ml/hr.

As for the above, the distance was maintained at 11 cm to gain the optimum applied voltage for the given distance. Therefore, aligning that applied voltage to that determined distance and analysing the subsequent fibre morphology. The goal of this was to see the change in voltage draw out a smooth, uninterrupted fibre with sufficient flight time to dry and collect on the grounded collector plate (Jaeger et al., 1998). As seen in figure 4.1, the balance between collector plate distance and spinneret tip was not found causing intense beading with minor fibre formation, therefore an extension of distance and applied voltage needed to be used.

Figure 4.1 highlights that and increased voltage can break through the surface tension and form fibres out of the solution as given by the figures 4.1 D & C. In these images, fibres are present, and beading is minimally reduced from the previous results of 10 kV and 12 kV. This confirms that the use of a higher applied voltage can form fibres with a highly concentrated solution. A way of reducing this beading could be to introduce a volatility to the solution.

Changing the neutral PBS to another organic solvent, which would make the solution more volatile and reduce the viscosity (Jaeger et al., 1998). However, this was not the purpose of this study. Instead, the use of neutral solvents will protect the collagen structure and create unchanged collagen deposition as stated by Zeugolis et al (2008).

Following on from the initial calibration testing at 11 cm. Adjustments were made in relation to the images seen in figure 4.1. The distance may have been too short to make an electrostatic pull on the sample but more of an electrostatic jump. This can be applied to the prevalence of beading in the collected images of the qualifying tests. The goal is to draw out the material at such a rate to enable smooth fibre diameter and minimal beading or spraying. While the amount of parameter adjustment is high, it enables a clear view on how each variable influences the fibre deposition. When considering the following tests, the focus moved to the Taylor cone formation in initiating uniform fibre flow.

At lower distances from the needle to collector, the movement of media was sudden. The formation of a Taylor cone in the end of the needle was not observed and instead the sample would jump across the distance in a spray fashion rather than maintaining its surface tension and flowing into a fibre. While increasing the distance increased the visible effects of the electrostatic force and enabled a Taylor cone to reach full formation. This could be seen while ramping up the voltage before the solution could travel across the gap. There was a considerable drop off after 18cm where the voltage was not affecting the solution and it was deemed unsafe to proceed increasing the electrical input. However, between the range of 14 – 17 cm the fibre formation was visible and allows for some successful trial runs.

At an increased distance, the voltage was adjusted accordingly to maintain the force across the gap and allow proper movement of media from the solution to the collector plate. In the process, the flow rate of the syringe was adjusted ad hoc to maintain a small droplet at the tip. The balance of all three key parameters was crucial in maintaining the flow of solution and not breaking the formation of non-woven fibres on the collector plate surface. Further adjustments were made until it was settled that 20 kV would be sufficient to pull the fibres

with minimal beading. This was done at 16 cm from the spinneret tip to the collector plate at a flow rate of 0.05 ml/hr. An example is found below in figure 4.2:

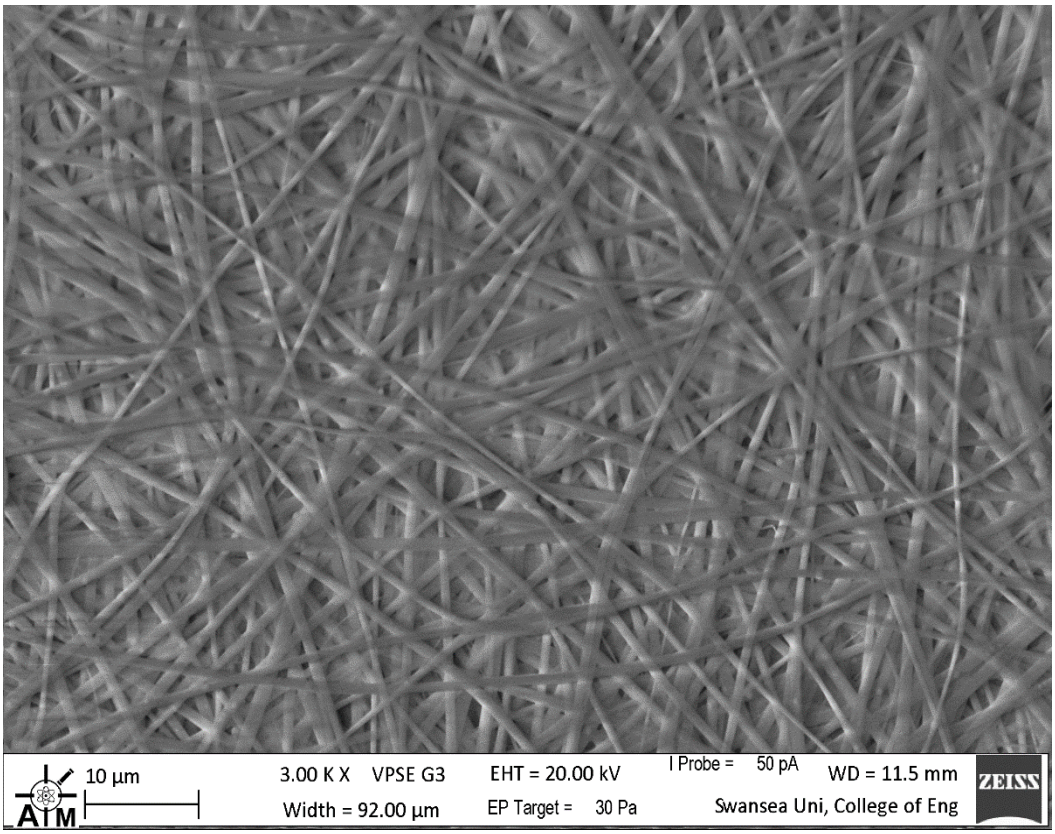

Figure 4.2 - SEM image of Electrospun Monomeric Collagen in PBS, spun at 20 kV, 0.05 ml/hr and at 16 cm

Figure 4.2 distinctly shows the fibre formation and overlay of dried fibres on top of one another. There is minor fibre diameter variation with a mean diameter of 0.759 µm – the standard deviation of the fibres is low at 0.153, which indicates that the fibres are being drawn and dried at an even rate across the distance. A total of three final mats were used to determine average fibre diameter for the fibres. Mat 1, 2 and 4. The mean diameter were 0.469, 0.679 and 0.759 µm respectively with low standard deviation in the range of 0.085 to 0.175 confirming the consistency of fibre diameter throughout eat electrospinning run. Confirmation of this process resulted in four collagen mats that could peel away from the aluminium foil and used in the Deben Micro Tensile Tester.

4.2 Hydroxyapatite

The hydroxyapatite precipitate was formed using three finishing methods; air dried, freeze dried and sintered. While the prior process remained the same. These were pressed onto carbon tape to be imaged using both the HDoF and SEM to see if rod like formation has evolved. The HDoF images are hard to see, however there is some disparity in particle shape between the three finishing methods.

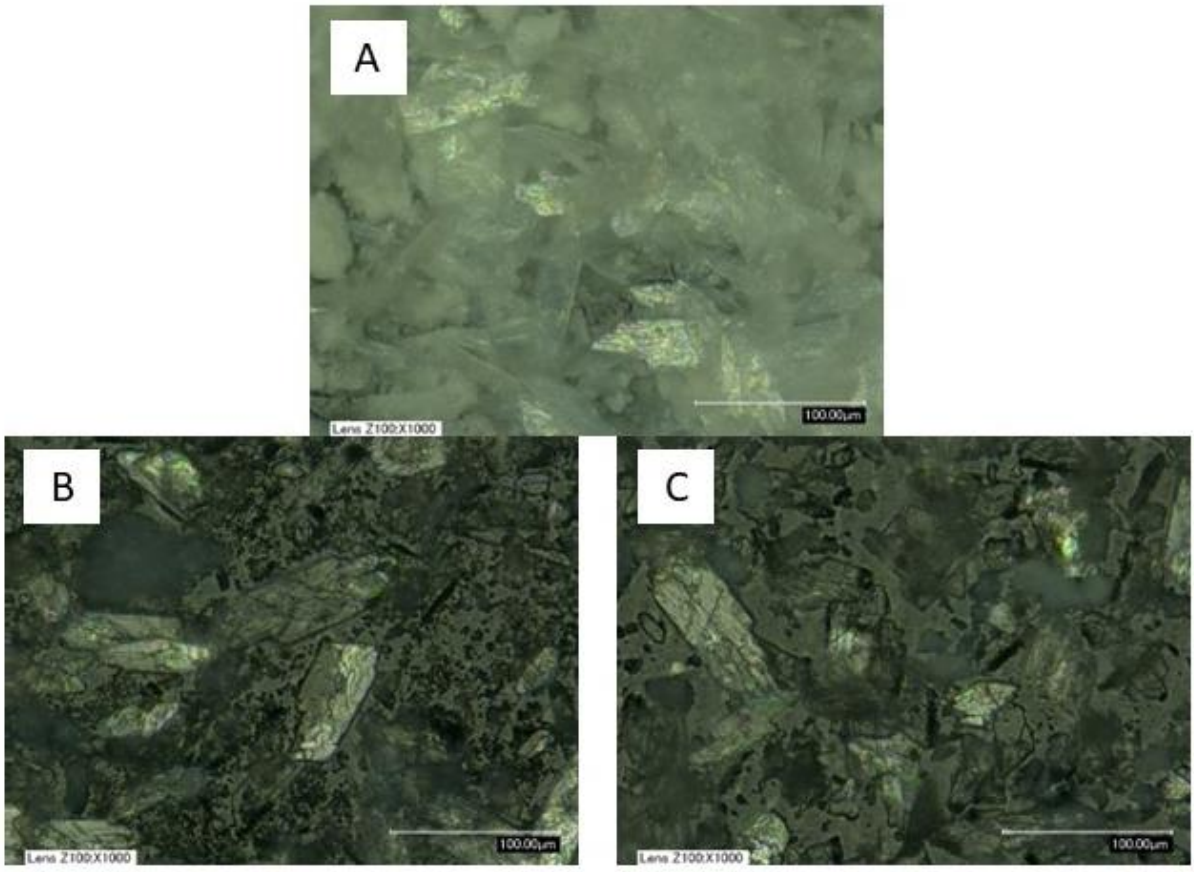

Figure 4.3 - High depth of field images of Hydroxyapatite after three finishing variations. A - Sintered at 30°C ramp up to 1100°C. B - Freeze dried. C - Air dried

Figure 4.3 displays the three different techniques in which hydroxyapatite can be finished through laboratory synthesis.

With the use of sintering, the particles stuck together more and as a result saturated the image gained from the microscope. However, from the image it can be seen that the particles tend towards an oval like shape. Sizes ranging between 50 µm to 80 µm. The particles are not rod like, instead they represent elongated shards which have enough binding sites in which a solution of collagen can wrap around it.

The freeze-dried method hold little change to air drying the precipitate into a powder form. The images clearly show that there is rod like structures, but very far and few apart. Many particles fall within the square and circular shape category. This does not indicate that hydroxyapatite did not form. Hydroxyapatite is formed by drying the precipitate therefore, hydroxyapatite was formed. The difference is the final morphology of the particles when

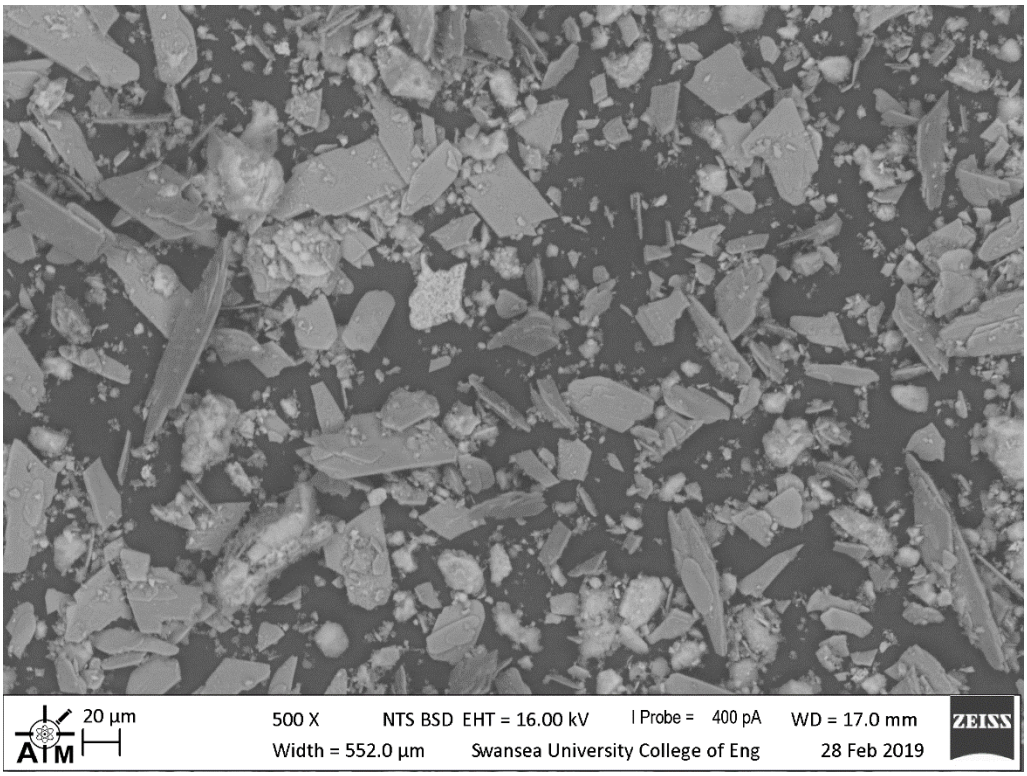

Figure 4.4 - SEM image of sintered hydroxyapatite showing a clear view of size and morphology.

introduced to a profound atmospheric change. Particle sizes rarely go above 50 µm and are irregularly shaped when compared to the sintering method.

In figure 4.4, the SEM depicts more elongated structures from the sintering process. For ease of comparison, the magnification of the SEM was set to a comparable setting to gain a much clearer vision of what was observed under the high depth of field microscope. It is clear that the shards theory is true. The variability between the particle sizes varies quite a lot from 100 µm to below 20 µm; however, there is a useable population of rod-like particles to use in practice.

To confirm the formation of hydroxyapatite further analysis came in the form of Fourier-transform infrared spectroscopy (FTIR) and X-Ray Diffraction (XRD). FTIR obtains the infrared absorption of the hydroxyapatite and the result seen in figure 4.5.

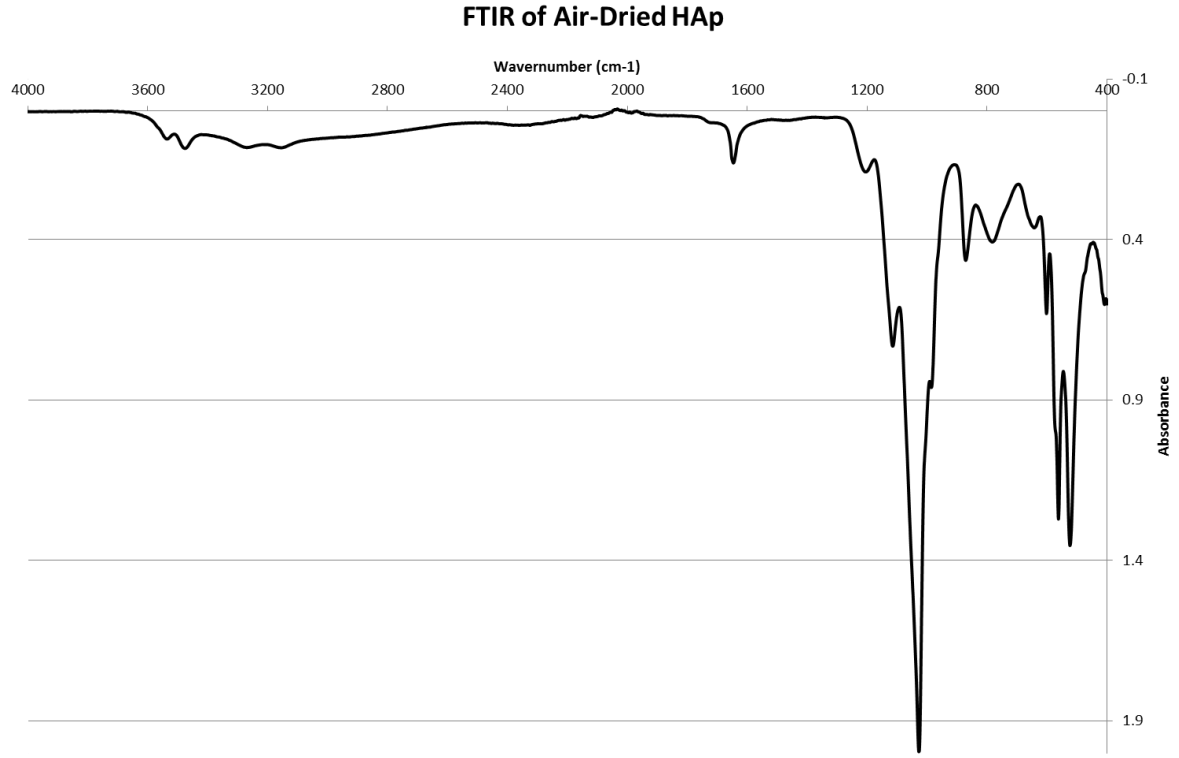

Figure 4.5 - FTIR spectrum of Air-Dried hydroxyapatite.

In figure 4.5, there are five distinct peaks found at approximately wavelength 500, 800, 1000, 1700 and 3500 cm^{-1}. As discussed by Jing et al (2012), the present expressions are found at 3577 cm^{-1}/636 cm^{-1} for OH-, PO_4^{3-} (deformation vibrations) between 560-600 cm^{-1}, CO_3^{2-} at 1400-1500 cm^{-1}/876 cm^{-1} and at 3400 cm^{-1}/1640 cm^{-1} H_2O. These same peaks can be explicitly seen on the figure above. With the most profound being at approximately 600 and 1000 cm^{-1}. For comparison, below (figure 4.6) is the FTIR spectrum Jing et al (2012) gathered:

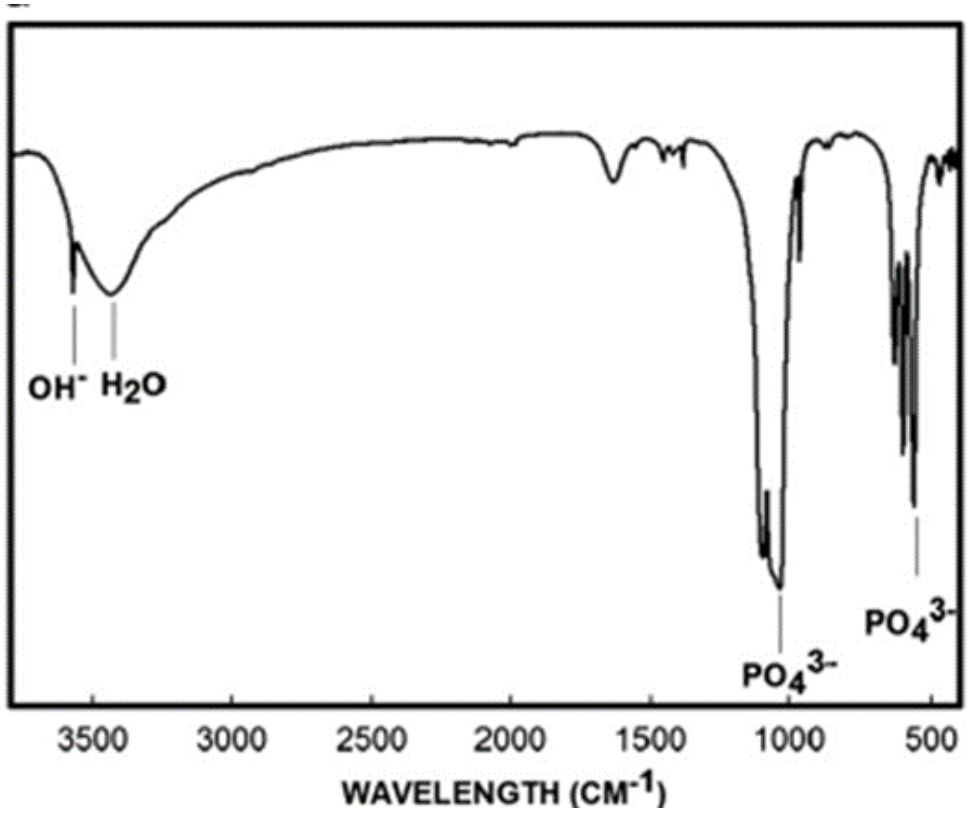

Figure 4.6 - FTIR spectrum of Nano hydroxyapatite (Jing et al., 2012)

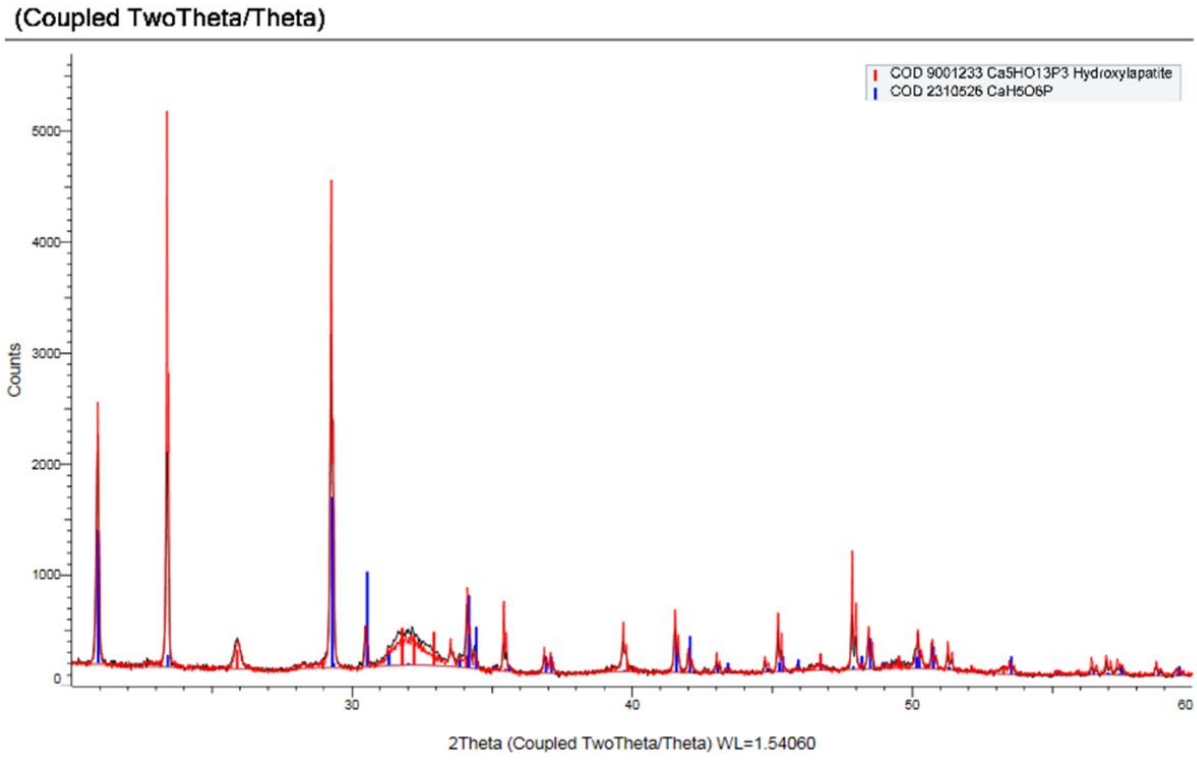

Figure 4.7 - XRD Pattern of Air-Dried hydroxyapatite

Figure 4.7 is an XRD pattern of the air-dried hydroxyapatite with respect to a controlled synthetic hydroxyapatite in red. The sample of laboratory air dried hydroxyapatite conforms well to the formula of hydroxyapatite ($Ca_5(PO_4)_3OH$). This confirms that the synthesised hydroxyapatite powder is hydroxyapatite.

The hydroxyapatite powder was introduced into a collagen solution ready for electrospinning. However, the sample run was unsuccessful due to the fast coagulation of the collagen with the hydroxyapatite.

4.3 Micro Testing

Tensile testing was performed using the Deben Micro tensile tester, I compared a collagen sponge with seven pieces of collagen mat spun at 20 kV, 0.05 ml/hr and at 16 cm from collector plate. All tested pieces measured 30 mm in length and 15 mm in width. The results are as shown in table 4-2:

	Thickness (mm)	Max Extension (mm)	Max Force (N)	UTS (N/mm^2)
MAT 1 (25% Single Alpha-Chain Collagen/1x PBS) (+10% wt HA)	0.11	0.142	0.8589	0.8031
MAT 2 (25% Single Alpha-Chain Collagen/1x PBS) (+10% wt HA)	0.11	0.200	0.7638	0.8402
MAT 3 (25% Single Alpha-Chain Collagen/1x PBS) (+10% wt HA)	0.14	0.655	0.0890	0.0810
MAT 4 (25% Single Alpha-Chain Collagen/1x PBS)	0.19	0.405	0.3132	0.1735
MAT 5 (25% Single Alpha-Chain Collagen/1x PBS)	0.16	0.270	0.7662	0.5041
MAT 6 (25% Single Alpha-Chain Collagen/1x PBS)	0.16	0.257	0.1852	0.1052

MAT 7 (25% Single Alpha-Chain Collagen/1x PBS)	0.16	0.263	0.1954	0.3439
Sponge 1	4.65	2.698	1.6439	0.040403
Sponge 2	4.65	2.009	1.2101	0.026501

Table 4-2 - Ultimate tensile strength, max force and other parameter taken from Deben Micro Tensile Testing

It is clear from table 4-2 that there is some disparity in resulted when looking at the strength of different thickness of mat. The collagen sponge was considerably stronger than the other mats. With repeatable 2 mm extension before breakage occurred and 1.2/1.6 N max force applied, the sponge is the stronger scaffold. However, the electrospun woven mats could achieve half the max force at 0.8589 N and 0.7638 N with limited extension of up to 0.2 mm. Mats 1 & 2 are stronger but brittle when a tensile force applied to them with a thinner overall profile. On the other hand, the thicker mats had more elasticity and stretch with Mat 3 reaching 0.655 mm at peak extension. Considering the sponge is 33 times thicker than the mat that is proportionally more elastic.

The Ultimate Tensile Strength (UTS) of the mats are considerably higher than those of the sponge for comparison. The thinner mats held up the best out of all of the other samples tested.

Following the mechanical testing, the samples were placed into the SEM to analyse the failure points. All were still connected at a point along the break and not fully broken apart.

Both figure 4.8 & 4.9 show sections of failure in the collagen material. The sponge shows a complete tear through the material however, because the material is thick, it is hard to visualise the result all the way through. The sponge is still more connected at the lower end of the image, showing a more elastic break when compared to Collagen mat 3.

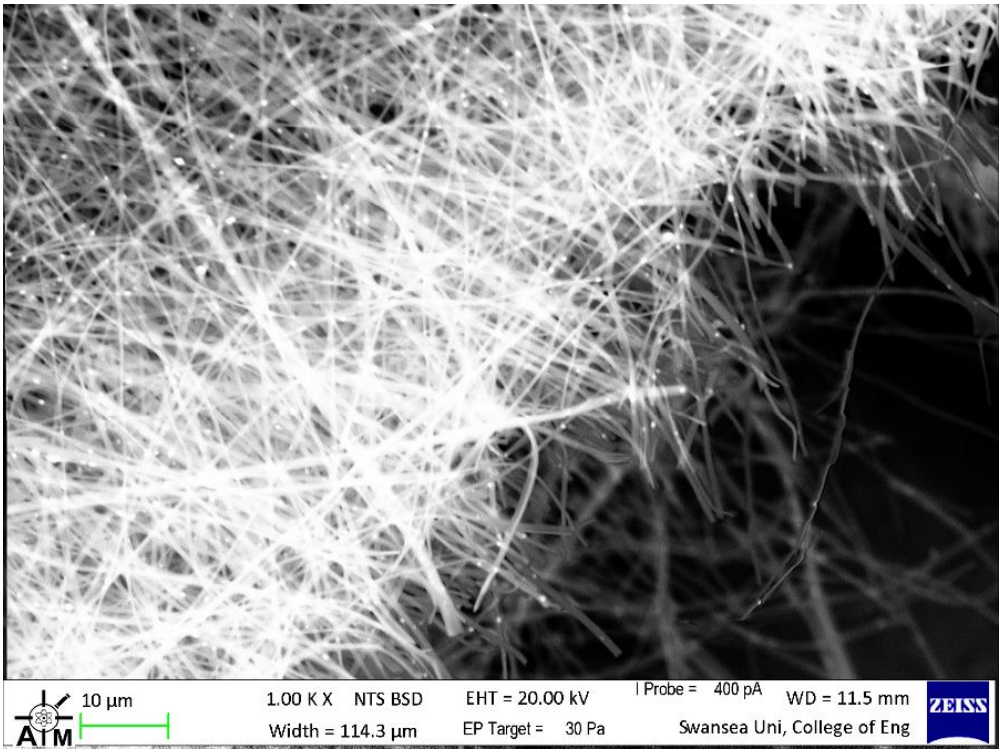

Figure 4.8 - SEM image of fibre breakage point seen on collagen mat 3 that was put under tensile load.

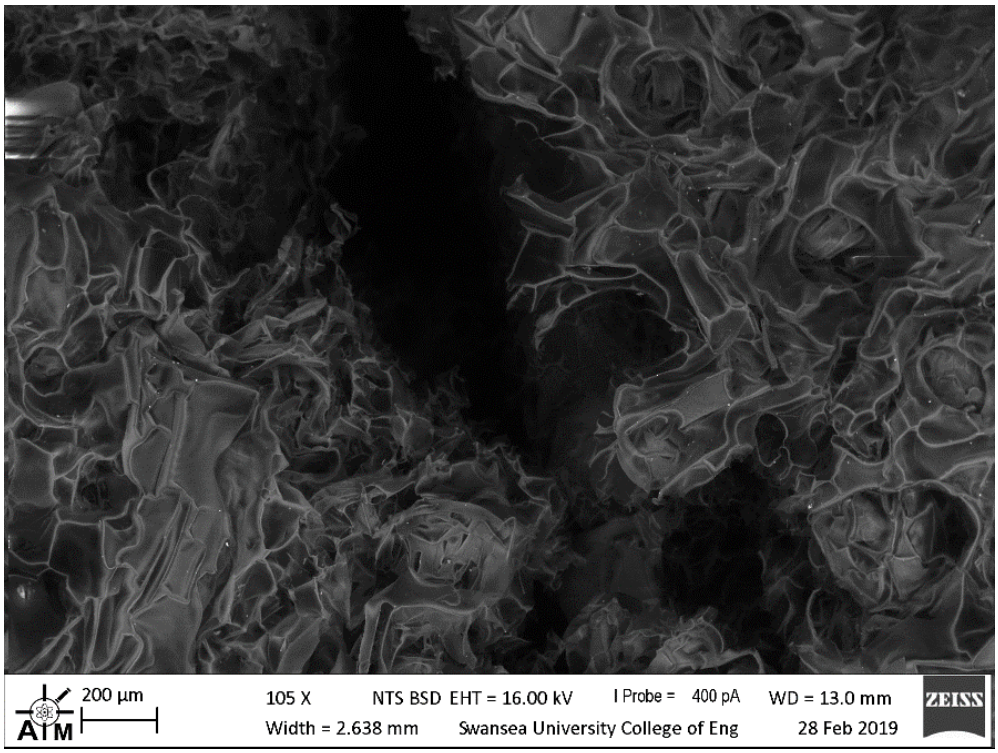

Figure 4.9 - Collagen sponge tear from tensile testing

Mat 3 shows a large point of failure where all of the fibres are snapped away from the rest of them. It can be seen to go throughout the thickness of the material and effect the entirety of the sample. The strength in the mat relies on the summation of individual fibres

however, once a failure occurs a cascading effect occurs. Therefore, we see such a clean separation between the collagen fibres.

Figure 4.8 - Force (N) against Time (s) curve comparing collagen mats with and without Hydroxyapatite additive.

When comparing the relative tensile strength of the electrospun collagen mats. I was able to evaluate how the use of Hydroxyapatite influenced the final mat. The maximum force seen in table 4-2 shows that the combination of collagen and hydroxyapatite produces a material that can withstand a higher load over the same area.

As is visible on figure 4.10 above, there is a clear discrepancy between the two collagen mats. The lines depict the force that is experienced by the mats over time until ultimate failure. The sample rate used in the tests were set to 100 ms intervals with the drive motor set to pull at a rate of 0.1 mm/minute. The high sample rate and slow speed was used to ensure that the load was applied evenly across the material without it running too fast which would have caused sudden tears without any proper tensioning on the material. The rate speed was chosen at 0.1 mm/minute to ensure that every fibre within the material could experience the strain for a sustained amount of time and allowing for natural breakage points and fault lines to arise.

When reflecting on figure 4.10, the difference in tensile strength between the two test materials is large. The orange line, representing the collagen mat with hydroxyapatite, it is

clear that under the same load rate of the micro-tensile tester it can experience a larger load over time. However, the material fails earlier at around 105 seconds. Although the rise in tension is not without interruption. As more tension was applied to the mat there is a small force dip at approximately 90 seconds – this could imply a fracture has occurred and an internal weakness has been exposed and broken. This could be the origin of the ultimate failure seen at the 105 second mark.

In contract to that, the blue line which represents an electrospun collagen mat with no additives displays a lack of internal strength. The reserved force it experiences can be a result in leak fibre bonding as the mat dried on the collector plate. This means that the fibres were constantly shifting and moving as the material was under tensile load. This opens the discussion for the elasticity of the material – allowing for increased mailability of the material and can be pressed and pulled into different shapes. A trend that is highlighted in figure 4.10 is the swift nature of deterioration from the initial failure point presenting itself to its ultimate failure.

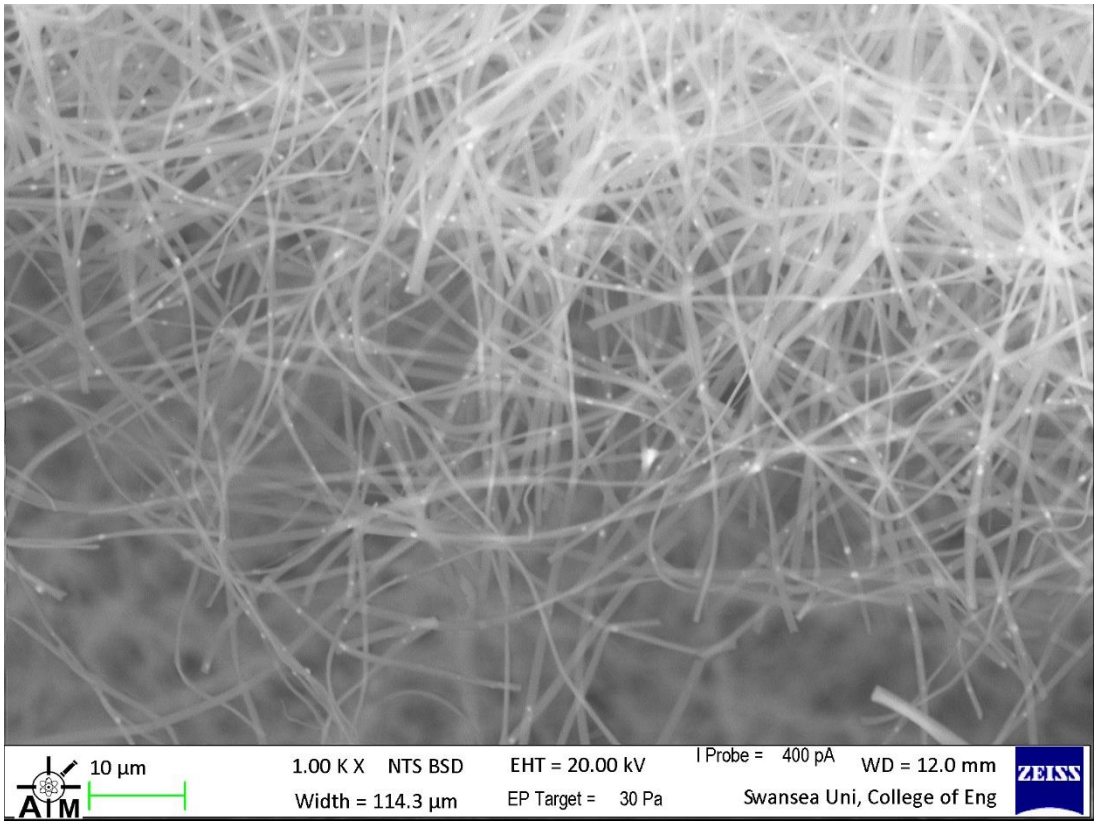

Figure 4.9 - SEM image of post tensile testing mat (collagen with 10% hydroxyapatite)

It seems that both mats experience a swift loss in tensile load as fibres break under load and then begin to sustain the reduced load before continuing to fail. This is an inherent nature

that can be attributed to the layered aspect of a non-woven mat. As some layers become weak and fail from the applied load, the layers that are not yet broken take up the slack but without the support of numerous fibres it will inevitably fail. An example of the layering can be seen in the above figure, figure 4.11. At 1000x magnification torn fibres can be seen as an example of the failure due to tensile load. However, the layers throughout the mat are effected differently. The top layers of fibres have torn dramatically although upon further inspection, the lower layers are visible and do not look visually different to a fresh mat. Upon further analysis of the materials used for tensile testing there are benefits and drawbacks to each non-woven mat constituents. Whereas the fibres that are imbued with hydroxyapatite presented more sustained load, the fibres can be seen as brittle and failing dramatically once a threshold point has been reached. In contrast, the collagen mat displayed more flexibility in its tensile ability and breaks could not be seen as substantial and instead minimal. The lack of calcium derived additive caused the fibres to roll over each other instead of forming together as a single layer.

5. Conclusion

The goal of this thesis was to use a neutral solvent to aid in the electrospinning of collagen as to not expose it to harsh solvents such as, fluoroalcohols and denature the material. The fibres that were produced involved a blend of 25% weight of Jellyfish Single Alpha-Chain collagen and 1x Phosphate Buffer Saline which when using in an electrospinning system at 20 kV, 0.05 ml/hr and 16 cm from the spinneret tip to collector plate. These fibres averaged a diameter of between 0.469 and 0.759µm. It was found through initial calibration that 11 cm was too short of a distance to allow for sufficient flight travel of the solution for fibres to form. Instead, the short distance provided the optimal conditions for beading and spraying to occur. It was noted that as the increased voltage was applied, the threshold voltage was being reached in order to overcome the high surface tension brought on by the high concentration solution. Due to the use of non-aggressive solvents, a higher concentration of collagen was needed to mimic the electrospinning of low concentrations with harsh fluoroalcohols. A study on the preparation and morphology of hydroxyapatite was conducted with varying results. It was observed that the use of sintering in the final steps of synthesis alters the particle morphology into more rod like shaped which when included into solution can provide strengthened mechanical properties and bioactive binding for bone regeneration. No observable difference was found when comparing freeze dried hydroxyapatite to the air dried. The methods are indistinguishable. To slow down the reaction between hydroxyapatite and collagen before electrospinning, a lower concentration is recommended. The hydroxyapatite binds too readily to the collagen in solution to which coagulation is almost immediate preventing the electrospinning process to go any further. The work conducted with the micro tensile tester proved that the woven mat compared to its thickness has comparable force to a sponge much denser. That said, it is still unclear as to how much affect the thickness of the mat has on the strength of the final product. However, the thickness has some influence on the elasticity as this could be due to more available fibres to break before it reached its UTS.

5.1 Further Work

The immediate coagulation of hydroxyapatite and collagen solutions is not ideal for electrospinning. A way of delaying this reaction can be researched. The powder is found naturally with collagen fibres to develop bone. However, reducing the coagulation speed will mean either reducing the concentration of the collagen within solution or experiment with mild solvents lower on the pH scale.

With fully formed mats, cell seeding can take place with research done into bio factors and binding site activation methods to increase the biocompatibility and versatility of the collagen woven mat.

Porosity of collagen scaffolds has not been examined. As collagen is the framework for which ECM's are formed, the ease of cell penetration would be beneficial to estimate growth rate within the scaffold or successful attachment to the site. Therefore, further investigation into the use of neutral solvents for hydroxyapatite and collagen electrospinning including cell seeding and biocompatibility.

6. References

1. Rho KS, Jeong L, Lee G, Seo B-M, Park YJ, Hong S-D, et al. Electrospinning of collagen nanofibers: effects on the behavior of normal human keratinocytes and early-stage wound healing. Biomaterials. 2006 Mar;27(8):1452–61. Available from: http://www.ncbi.nlm.nih.gov/pubmed/16143390

2. CHAFFEY N. Alberts, B., Johnson, A., Lewis, J., Raff, M., Roberts, K. and Walter, P. Molecular biology of the cell. 4th edn. Ann Bot. 2003 Feb 1;91(3):401–401. Available from: https://academic.oup.com/aob/article-lookup/doi/10.1093/aob/mcg023

3. Petreaca M, Martins-Green M. The Dynamics of Cell-ECM Interactions, with Implications for Tissue Engineering. In: Principles of Tissue Engineering [Internet]. Elsevier; 2014. p. 161–87. Available from: http://linkinghub.elsevier.com/retrieve/pii/B9780123983589000094

4. Patino MG, Neiders ME, Andreana S, Noble B, Cohen RE. Collagen: an overview. Implant Dent. 2002;11(3):280–5. Available from: http://www.ncbi.nlm.nih.gov/pubmed/12271567

5. Sun Z, Zussman E, Yarin AL, Wendorff JH, Greiner A. Compound Core–Shell Polymer Nanofibers by Co-Electrospinning. Adv Mater. 2003 Nov 17;15(22):1929–32. Available from: http://doi.wiley.com/10.1002/adma.200305136

6. Sapountzi E, Braiek M, Farre C, Arab M, Chateaux J-F, Jaffrezic-Renault N, et al. One-Step Fabrication of Electrospun Photo-Cross-Linkable Polymer Nanofibers Incorporating Multiwall Carbon Nanotubes and Enzyme for Biosensing. J Electrochem Soc. 2015 Aug 12;162(10): B275–81. Available from: http://jes.ecsdl.org/lookup/doi/10.1149/2.0831510jes

7. Teng SH, Lee EJ, Wang P, Kim HE. Collagen/hydroxyapatite composite nanofibers by electrospinning. Mater Lett. 2008 Jun 30;62(17–18):3055–8.

8. Hua FJ, Kim GE, Lee JD, Son YK, Lee DS. Macroporous poly(L-lactide) scaffold 1. Preparation of a macroporous scaffold by liquid–liquid phase separation of a PLLA–dioxane–water system. J Biomed Mater Res. 2002 Jan 1;63(2):161–7. Available from: https://onlinelibrary.wiley.com/doi/full/10.1002/jbm.10121

9. Burgeson RE, Nimni ME. Collagen types. Molecular structure and tissue distribution. Clin Orthop Relat Res. 1992 Sep;(282):250–72. Available from: http://www.ncbi.nlm.nih.gov/pubmed/1516320

10. Zong X, Kim K, Fang D, Ran S, Hsiao BS, Chu B. Structure and process relationship of electrospun bioabsorbable nanofiber membranes. Polymer (Guildf). 2002 Jun 10;43(16):4403–12.

11. Kidoaki S, Kwon IK, Matsuda T. Mesoscopic spatial designs of nano- and microfiber meshes for tissue-engineering matrix and scaffold based on newly devised multilayering and mixing electrospinning techniques. Biomaterials. 2005 Jan;26(1):37–46. Available from: http://www.ncbi.nlm.nih.gov/pubmed/15193879

12. Hong DP, Hoshino M, Kuboi R, Goto Y. Clustering of fluorine-substituted alcohols as a factor responsible for their marked effects on proteins and peptides. J Am Chem Soc. 1999 Sep 22;121(37):8427–33.

13. Li Z, Wang C. Effects of Working Parameters on Electrospinning. In 2013. p. 15–28.

14. Zhang YZ, Venugopal J, Huang Z-M, Lim CT, Ramakrishna S. Characterization of the surface biocompatibility of the electrospun PCL-collagen nanofibers using fibroblasts. Biomacromolecules;6(5):2583–9. Available from: http://www.ncbi.nlm.nih.gov/pubmed/16153095

15. Super-Hydrophobic Surface of Aligned Polyacrylonitrile Nanofibers - Feng - 2002 - Angewandte Chemie International Edition - Wiley Online Library. Available from: https://onlinelibrary.wiley.com/doi/10.1002/1521-3773(20020402)41:7%3C1221::AID-ANIE1221%3E3.0.CO;2-G

16. Yarin AL, Koombhongse S, Reneker DH. Taylor cone and jetting from liquid droplets in electrospinning of nanofibers. J Appl Phys. 2001 Nov 16;90(9):4836–46. Available from: http://aip.scitation.org/doi/10.1063/1.1408260

17. Petreaca M, Martins-Green M. The Dynamics of Cell-ECM Interactions, with Implications for Tissue Engineering. In: Principles of Tissue Engineering: Fourth Edition. Elsevier Inc.; 2013. p. 161–87.

18. Athanasiou KA, Eswaramoorthy R, Hadidi P, Hu JC. Self-Organization and the Self-Assembling Process in Tissue Engineering. Annu Rev Biomed Eng. 2013 Jul; 15:115. Available from: /pmc/articles/PMC4420200/

19. Bajáková J, Chaloupek J, Lukáš D, Lacarin M. "DRAWING"-THE PRODUCTION OF INDIVIDUAL NANOFIBERS BY EXPERIMENTAL METHOD. 2011.

20. Deitzel JM, Kleinmeyer J, Harris D, Beck Tan NC. The effect of processing variables on the morphology of electrospun nanofibers and textiles. Polymer (Guildf). 2001;42(1):261–72.

21. Ondarçuhu T, Joachim C. Drawing a single nanofibre over hundreds of microns. Europhys Lett. 1998 Apr 1;42(2):215–20. Available from: https://epljournal.edpsciences.org/articles/epl/abs/1998/08/42218/42218.html

22. McManus MC, Boland ED, Simpson DG, Barnes CP, Bowlin GL. Electrospun fibrinogen: feasibility as a tissue engineering scaffold in a rat cell culture model. J Biomed Mater Res A. 2007 May;81(2):299–309. Available from: http://www.ncbi.nlm.nih.gov/pubmed/17120217

23. Ji J, Bar-On B, Wagner HD. Mechanics of electrospun collagen and hydroxyapatite/collagen nanofibers. J Mech Behav Biomed Mater. 2012 Sep; 13:185–93. Available from: http://www.ncbi.nlm.nih.gov/pubmed/22906988

24. Jaeger R, Bergshoef MM, Martín I Batlle C, Schönherr H, Vancso GJ. Electrospinning of ultra-thin polymer fibers. Macromol Symp. 1998; 127:141–50.

25. Buttafoco L, Kolkman NG, Engbers-Buijtenhuijs P, Poot AA, Dijkstra PJ, Vermes I, et al. Electrospinning of collagen and elastin for tissue engineering applications. Biomaterials. 2006 Feb;27(5):724–34.

26. Fratzl P, Gupta HS, Paschalis EP, Roschger P. Structure and mechanical quality of the collagen-mineral nano-composite in bone. Vol. 14, Journal of Materials Chemistry. 2004. p. 2115–23.

27. Yi F, LaVan DA. Poly(glycerol sebacate) Nanofiber Scaffolds by Core/Shell Electrospinning. Macromol Biosci. 2008 Sep 9;8(9):803–6. Available from: http://doi.wiley.com/10.1002/mabi.200800041

28. Patient education: Coronary artery bypass graft surgery (Beyond the Basics) - UpToDate. Available from: https://www.uptodate.com/contents/coronary-artery-bypass-graft-surgery-beyond-the-basics/print

29. Petrik S, Maly M. Production Nozzle-Less Electrospinning Nanofiber Technology. MRS Proc. 2009 Jan 31; 1240:1240-WW03-07. Available from: https://www.cambridge.org/core/product/identifier/S1946427400021606/type/journal_article

30. Niu H, Wang X, Lin T. 15+ MILLION TOP 1% MOST CITED SCIENTIST 12.2% Chapter from the book Nanofibers-Production, Properties and Functional Applications Downloaded from: http://www.intechopen.com/books/nanofibers-production-properties-and-functional-applications 2 Needleless Electrospinning: Developments and Performances. Available from: www.intechopen.com

31. Yang L, Fitié CFC, van der Werf KO, Bennink ML, Dijkstra PJ, Feijen J. Mechanical properties of single electrospun collagen type I fibers. Biomaterials. 2008 Mar;29(8):955–62.

32. Zhang C, Yuan X, Wu L, Han Y, Sheng J. Study on morphology of electrospun poly(vinyl alcohol) mats. Eur Polym J. 2005 Mar;41(3):423–32.

33. Huang Z-M, He C-L, Yang A, Zhang Y, Han X-J, Yin J, et al. Encapsulating drugs in biodegradable ultrafine fibers through co-axial electrospinning. J Biomed Mater Res Part A. 2006 Apr;77A(1):169–79. Available from: http://www.ncbi.nlm.nih.gov/pubmed/16392131

34. Ramakrishna S, Fujihara K, Teo W-E, Lim T-C, Ma Z. An Introduction to Electrospinning and Nanofibers. WORLD SCIENTIFIC; 2005. Available from: http://www.worldscientific.com/worldscibooks/10.1142/5894

35. Petrik S, Maly M. Production Nozzle-Less Electrospinning Nanofiber Technology. MRS Proc. 2009 Jan 31; 1240:1240-WW03-07. Available from: https://www.cambridge.org/core/product/identifier/S1946427400021606/type/journal_article

36. Agarwal S, Wendorff JH, Greiner A. Use of electrospinning technique for biomedical applications. Vol. 49, Polymer. Elsevier; 2008. p. 5603–21. Available from: http://www.sciencedirect.com/science/article/pii/S0032386108007994

37. Lee JK, Link JM, Hu JCY, Athanasiou KA. The Self-Assembling Process and Applications in Tissue Engineering. Cold Spring Harb Perspect Med. 2017 Nov 1;7(11). Available from: /pmc/articles/PMC5666628/

38. Zeugolis DI, Khew ST, Yew ESY, Ekaputra AK, Tong YW, Yung L-YL, et al. Electro-spinning of pure collagen nano-fibres - just an expensive way to make gelatin? Biomaterials. 2008 May;29(15):2293–305. Available from: http://www.ncbi.nlm.nih.gov/pubmed/18313748

39. Yu X, Zhang H, Miao Y, Xiong S, Hu Y. Recent strategies of collagen-based biomaterials for cartilage repair: from structure cognition to function endowment. J Leather Sci Eng. 2022;4(1). Available from: https://doi.org/10.1186/s42825-022-00085-4

40. Di J, Zhao Y, Yu J. Fabrication of molecular sieve fibers by electrospinning. J Mater Chem. 2011 Jun 6;21(24):8511. Available from: http://xlink.rsc.org/?DOI=c1jm10512d